Paramagnetic Resonance of Fe^{3+} in $CdGa_2Se_4$ Crystals

D. Siebert and S. Febbraro
Institut für Physikalische Chemie, Universität Freiburg i. Br.

Z. Naturforsch. **42 a**, 258–262 (1987); received November 28, 1986

Fe^{3+} may serve as a substitutional spin probe to characterize the two different Ga sites in $CdGa_2Se_4$. Unusually high tilting angles are found for the Fe^{3+} centers and indicate the limits for applying the spin probe technique.

1. Introduction

$CdGa_2Se_4$ is a representative of the well known defect chalcopyrite structures of space group $I\bar{4}$ (thiogallate structures), which are very promising because of their optical and electrical properties [1, 2]. The unit cell contains two crystallographically different Ga sites, both at special positions with local symmetry $\bar{4}$ and tetrahedrally coordinated by four anions. Formerly we investigated the EPR of Fe^{3+} as spin probes in $CdGa_2S_4$ to characterize the corresponding different Ga sites, and found besides a strongly axial center an almost cubic one [3]. The question arose, if this was a characteristic mark of the thiogallate structures. Furthermore the utility of Fe^{3+} as a spin probe shall be examined.

2. Crystal Growth and Iron Doping

The crystals were grown in evacuated quartz ampoules by chemical vapour transport using iodine as transport agent. Starting materials were Ga_2Se_3, obtained by direct synthesis of the elements, CdSe, and small amounts of iron powder. All elements and CdSe were of 5N purity. The temperature of the hot and cold end of the ampoule was kept at 650 °C and 605 °C respectively. After five days crystals of different size were obtained, often with (112), (11$\bar{2}$), and (001) faces. Whereas pure $CdGa_2Se_4$ crystals are reddish brown and transparent, the colour of the Fe-doped crystals became darker with increasing iron content, and are already black at 1% Fe-doping (atomic percent with respect to Ga). In order to investigate the broad Fe^{3+} signals fairly well, doping with 0.3% to 1% Fe was necessary, indicating that much of the iron will be in the divalent state.

Reprint requests to Prof. Dr. D. Siebert, Institut für Physikalische Chemie, Albertstr. 21, D-7800 Freiburg i. Br.

3. EPR Measurements, Evaluation of the EPR Parameters

The measurements were performed with a microwave frequency of 34.9 GHz, mostly on a 1% iron-doped small plate of about $4 \times 2 \times 1\ mm^3$ with (112), (11$\bar{2}$), and (001) faces. The reasonance fields did not show any differences compared to those obtained with some other crystals doped with 0.3 and 0.5%. Due to the local symmetry $\bar{4}$ the following spin-Hamiltonian was used for $S = 5/2$:

$$\mathcal{H} = g_\parallel \beta H_z S_z + g_\perp \beta (H_x S_x + H_y S_y) + B_2^0 O_2^0 + B_4^0 O_4^0 + B_4^4 O_4^4 . \quad (1)$$

For cubic symmetry B_4^0 equals $(1/5)\,B_4^4$. Therefore the difference $B_4^{0'} = B_4^0 - (1/5)\,B_4^4$ will be a measure for the deviation from cubic symmetry. Very often one may neglect the last term in (1), especially for $H \parallel z$, and then the Hamiltonian is diagonal within the manifold of the spin functions $|M\rangle$. Therefore the resonance fields follow from differences of the diagonal elements, and the parameters $g_\parallel$, B_2^0, and B_4^0 are directly obtained from the positions of the EPR lines.

The spectrum for $H \parallel c \parallel z$ is shown in Figure 1 a. The lines for low and medium fields indicate that the Zeeman energy is comparable with the zero-field splitting. The spectrum can be understood, if one assumes two different Fe^{3+} centers with dominant axial parameters B_2^0. There are three signals I, associated with one center I because of their nearly

0340-4811 / 87 / 0300-0258 $ 01.30/0. – Please order a reprint rather than making your own copy.

equal distances (about $6B_2^0/g_\parallel\beta$) and their decreasing intensities towards lower magnetic fields. The remaining two lines show the opposite intensity behaviour and are therefore due to another center II with greater B_2^0, so that the line at about 0.9 T is the 'reflected' one (reflected at zero magnetic field). For both centers the transitions $-1/2 \rightarrow 1/2$ overlap. The high-field resonances beyond this transition are missing because they occur above the field range of our magnet. After this assignment of the lines the values for $g_\parallel$, B_2^0, and B_4^0 can be determined immediately from the resonance fields of Fig. 1a for both centers (Table 1). The accuracy is limited mainly by the broadness of the lines (0.009–0.035 T).

In order to obtain B_4^4 and $g_\perp$, another orientation of the magnetic field has to be chosen, preferably $H \perp z$, i.e. H in the a, b-plain (Figure 1b). The assignment of the lines to the centers I and II was possible by numerical calculations of the resonance fields, using the already existing parameters B_2^0, B_4^0, and setting $g_\perp = g_\parallel$, $B_4^4 = 0$ in Equation (1). These calculations were performed by exact numerical diagonalization of the spin-Hamiltonian matrices.

The experimental resonance fields for the angular variation in the a, b-plain are displayed in Fig. 2 for two selected lines of center I and one line of center II, together with the positions of a Mn^{2+} sextet, which was detectable from inherent Mn impurities. The evaluation of B_4^4 followed from the difference of the extreme resonance fields, which occur along a single curve of Figure 2. Such a difference ΔH will not depend strongly on $g_\perp$ and is proportional to B_4^4, as demonstrated in Fig. 3, where calculated differences ΔH are plotted versus assumed values of B_4^4 for one selected line of center I and II, respectively. It is noteworthy that for this evaluation of B_4^4 one doesn't need to know the orientation of the EPR axes x and y for the Hamiltonian (1) within the a, b-plain. It is clear by arguments of symmetry that the extrema of the resonance fields in this plain will occur if the magnetic field points to x-direction for one extremum and if it is rotated through 45° for the other extremum. The evaluation of B_4^4 was possible in the described manner for center I by means of the two different resonance lines of Fig. 2 and yielded the same value. Finally $g_\perp$ was varied

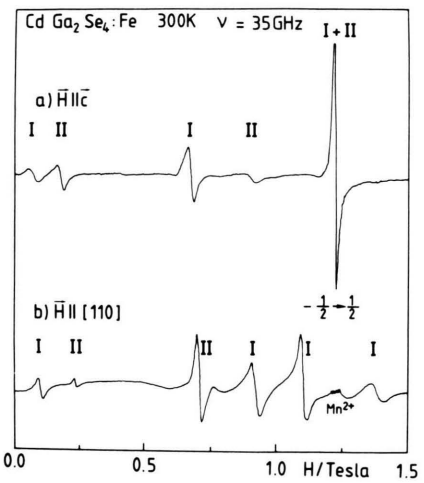

Fig. 1. ESR of $CdGa_2Se_4$: Fe, a) $H \parallel c$, b) $H \parallel [110]$. I and II denote resonances of center I and II, respectively.

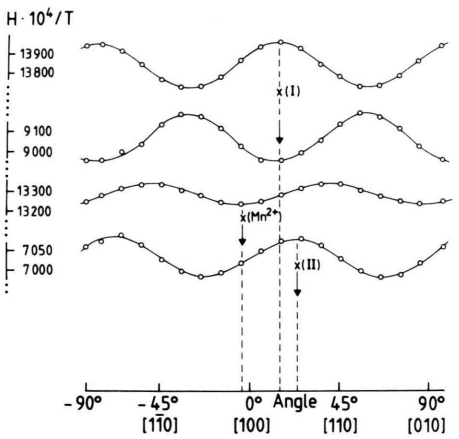

Fig. 2. Angular dependence in the a, b-plain. From top to bottom: Two selected resonances of center I, one Mn^{2+} sextet, and one line of center II.

Table 1. EPR parameters for Fe^{3+}(I) and Fe^{3+}(II) in $CdGa_2Se_4$; energies are given in $10^{-4}\,cm^{-1}$, τ (EPR) in degree.

Center	$g_\parallel$	$g_\perp$	B_2^0	B_4^0	B_4^4	$B_4^{0\prime}$	τ (EPR)
I	2.0377(2)	2.040(1)	902(2)	0.60(1)	3.4(1)	−0.08(1)	15(1)
II	2.0377(2)	2.039(1)	−1676(2)	−0.38(1)	2.0(1)	−0.78(2)	23(1)

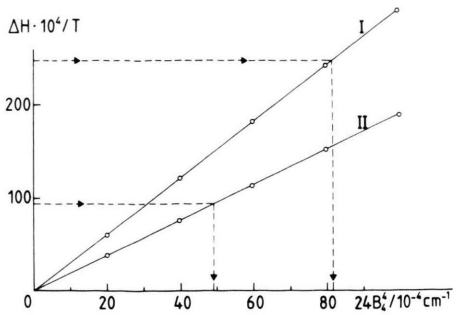

Fig. 3. Determination of B_4^4.

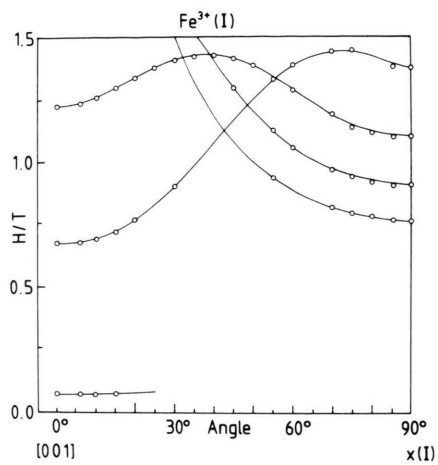

Fig. 4. Angular dependence for center I in the plain $c - x$.

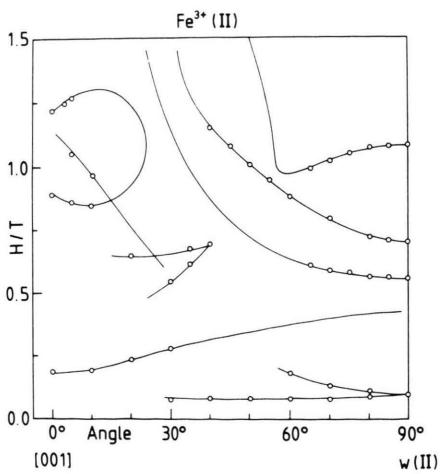

Fig. 5. Angular dependence for center II in the plain $c - w$ (see text).

until calculated extreme resonance fields fit the experimental ones.

The determination of the x, y-axes in the a, b-plain was possible for center I from Figure 2. The direction of one extreme resonance field pointed nearly towards $\{100\}$, the deviation being $\tau = 15°$, for the two uppermost curves of Figure 2. Therefore this direction was attached to the x-axis (or equivalent y-axis) of center I. By comparison with a cubic tetrahedral structure we fixed $B_4^4 > 0$. Then the sign for B_2^0 followed to be positive also. In $CdGa_2Se_4$ the ligand tetrahedra around the Ga atoms are rotated in the same direction with regard to $\{100\}$, [4], therefore the x-axis for center II should be rotated in this direction too. This argument yielded the position of the x(II)-axis, forming an angle of $\tau = 23°$ towards $\{100\}$. Assuming $B_4^4 > 0$ as for center I, B_2^0 turns out to be negative for center II.

With the parameters of Table 1 the angular dependence of the magnetic field at resonance was calculated in the plain [001]-x for center I, and [001]-w for center II, where w denotes the direction in middle of x and y. These plains were chosen because the resonance lines were sharpest here (cf. Discussion). The agreement between calculated and experimental resonance fields is very good, as demonstrated in Figs. 4 and 5.

Discussion

A structure refinement of $CdGa_2Se_4$ was recently reported [4]. Thereafter the $Ga(1)-Se_4$ tetrahedron is elongated along c whereas the $Ga(2)-Se_4$ tetrahedron is strongly compressed. A measure for the deviation from cubic symmetry is $3\cos^2\Theta - 1$, where the polar coordinate Θ denotes the angle of the bond direction towards the $\bar{4}$ axis. This expression equals zero for a regular tetrahedron, it is greater or smaller than zero, if the ligand tetrahedron is elongated or compressed, respectively. Besides this distortion from cubic symmetry the ligand tetrahedra are rotated through an angle τ (crystallographic tilting angle) about the $\bar{4}$ axis, compared to the position in an idealized structure, for which the positional parameters x and y of the ligands have the same value of 1/4.

Structural parameters for $CdGa_2Se_4$ are listed in Table 2, together with EPR parameters that shall be correlated. B_2^0 for Mn^{2+} is taken from [5].

Table 2. Comparison of structural properties and EPR parameters of Fe^{3+} and Mn^{2+} in $CdGa_2Se_4$ and $CdGa_2S_4$.

	$3\cos^2\Theta - 1$	τ (cryst)		$10^4 B_2^0/cm^{-1}$	τ (EPR)
$CdGa_2Se_4$					
Ga(1)	0.154	2.0°	Fe^{3+}(I)	902	15°
Ga(2)	− 0.267	3.8°	Fe^{3+}(II)	− 1676	23°
Cd	− 0.035	− 1.7°	Mn^{2+}	− 306	− 4°
$CdGa_2S_4$					
Ga(1)	0.029	0.8°	Fe^{3+}(I)	− 56	−
Ga(2)	− 0.249	1.1°	Fe^{3+}(II)	− 2095	−
Cd	− 0.023	− 0.8°	Mn^{2+}	− 75	−

In $CdGa_2Se_4$ there is a rough proportionality between $3\cos^2\Theta - 1$ of the unperturbed Ga sites and B_2^0 for center I and center II respectively. This is in agreement with the superposition model of Newman and Urban [6], and therefore we assign center I to Ga(1) and center II to Ga(2).

In Table 2 also values for $CdGa_2S_4$ are summarized from [3]. The almost cubic Fe^{3+} center in this crystal turns out to be a special feature of this representative and is not found in $CdGa_2Se_4$. But in both thiogallates the ligands of Ga(2) form a compressed tetrahedron, so that Ga(2) has definitely stronger axial character than Ga(1). This results in a pronounced negative B_2^0 of the same order of magnitude for both thiogallates. The strongly axial character of Ga(2) can also be understood by a simple point-charge model that considers the contributions of the four ligands and the next eight cations to the second-order crystal field, as published in [3].

The greater value of 2.038 for $g_\parallel$ of Fe^{3+} in $CdGa_2Se_4$ compared to 2.014 in $CdGa_2S_4$ (cf. [3]) can be explained in view of the greater covalency of the selenide.

The modulus of $B_4^{0\prime}$ that equals zero for a local cubic environment, turns out to be larger for the more axial center II, as one would expect. But there is no proportionality to the deviation from cubic symmetry, expressed by $3\cos^2\Theta - 1$.

Discrepancies between tilting angles of the unperturbed structure, called τ (cryst), and tilting angles of the associated paramagnetic center, called τ (EPR), were already reported for chalcopyrite structures [7]. Always τ (EPR) turned out to be larger than τ (cryst), and the differences increase in general with increasing τ (cryst). The greatest discrepancy reported in [7] was τ (cryst) = 6.9° for Ga^{3+} in $AgGaS_2$ compared to τ (EPR) = 10.9° for the associated Fe^{3+} center. It may be plausible that in a defect chalcopyrite structure greater values for τ (EPR) may occur, because the anions are only bound to three coordinated neighbours. But one hardly can imagine that the ligand tetrahedra around Fe^{3+} are rotated through 19° with respect to the tetrahedra around Ga^{3+}. So the reasons for the large tilting angles, measured by EPR, are not clear. A rather artificial explanation would be as follows: Not only the ligand tetrahedra around Fe^{3+} are rotated but also the particles of a larger surroundings, whereat this rotation decreases with increasing distance from the central impurity ion. In any case the large τ (EPR) is not a feature of the unperturbed structure but of the impurity center itself.

Special attention should be directed to the large line widths of the Fe^{3+} centers in $CdGa_2Se_4$ that range from 0.015 T to 0.06 T and are strongly dependent on the direction of the magnetic field, especially within the a, b-plain. This is shown in Fig. 6, where line widths are indicated by bars for center I at special directions of the magnetic field. The dependence on the field direction can be explained by a small additional rhombic term $B_2^2 O_2^2$ in (1) that varies statistically from one center to another. These rhombic terms have to be assigned to new x, y-axes, which are rotated through ± 45° with respect to the old ones. For $B_2^2 = 0.01\, B_2^0$ resonance fields were calculated and plotted in Fig. 6 resulting in two limiting curves for each resonance line. The plot shows that the rhombic term operates quite different upon the different resonance lines, and has no influence at special directions of the magnetic field. For these directions the observed line width must be smallest

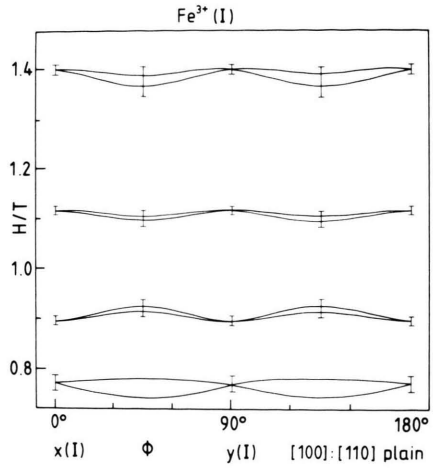

Fig. 6. Angular dependence for center I in the a, b-plain and line widths (see text).

and is indeed so. The line width increases with increasing difference between the limiting curves. So, for the lowest resonance line in Fig. 6, the resonance signal disappears, if one moves away from the special directions.

To explain the existence of a small rhombic term in (1) we propose the following model: The Fe^{3+} ions are displaced from the positions of the corresponding Ga ions, alternating in positive and negative directions along the c axis of the crystal. By that, two magnetically non-equivalent centers are formed whose x and y axes are interchanged and have the required directions, rotated through $\pm 45°$ compared to the old x, y-axes.

It should be mentioned that at X-band frequencies no EPR of the Fe^{3+} ions could be observed at room temperature for $CdGa_2Se_4$ in contrast to $CdGa_2S_4$. The reason for this will be the small perturbing term $B_2^2 O_2^2$ that has more influence at X-band frequencies, because of the smaller Zeeman interaction and the smaller microwave energy. On the other hand the Mn^{2+} resonances can be observed for both crystals at X-band and Q-band frequencies with quite normal and similar line widths of about 0.0025 T. This confirms our model, whereafter the peculiarities of the Fe^{3+} resonances in $CdGa_2Se_4$ mentioned above do not reflect properties of the unperturbed crystal but are due to the perturbing Fe^{3+} center itself*. With that, the limits of the spin probe technique are indicated, if one uses Fe^{3+} as a substitutional spin probe for Ga^{3+} in thiogallates. In this sense Mn^{2+} substituted for Cd^{2+} or Zn^{2+} seems to be more suitable. A comparison of Mn^{2+} centers detected by EPR in various thiogallates will be published in a forth-coming paper.

Acknowledgements

Calculations were performed on the Sperry 1100 computer of the Rechenzentrum der Universität Freiburg. We highly acknowledge the support of the Deutsche Forschungsgemeinschaft.

* *Note added in proof:* In the meantime we could perform measurements of the Ga NMR that indicate a small rhombic distortion of the Ga sites already in the undoped crystals.

[1] A. Miller, A. MacKinnon, and D. Weaire, Sol. State Phys. **36,** 119 (1981).
[2] A. MacKinnon, in: Festkörperprobleme XXI, ed. J. Treusch, Vieweg, Braunschweig 1981.
[3] B. Frick and D. Siebert, Z. Naturforsch. **37a,** 1005 (1982).
[4] V. Krämer, D. Siebert, and S. Febbraro, Z. Kristallogr. **169,** 283 (1984).
[5] M. Schlaak and A. Weiss, Z. Naturforsch. **27a,** 1624 (1972).
[6] D. J. Newman and W. Urban, Adv. Phys. **24,** 793 (1975).
[7] G. Brandt, A. Räuber, and J. Schneider, Sol. State Comm. **12,** 481 (1973).